A New Framework of Filter Bank Multi-Carrier: Getting Rid of Subband Orthogonality

Jian Dang, *Member, IEEE*, Zaichen Zhang, *Senior Member, IEEE*,
Liang Wu, *Member, IEEE*, and Yongpeng Wu, *Senior Member, IEEE*

***Abstract*— Filter bank multi-carrier (FBMC) entitles many advantages over orthogonal frequency division multiplexing (OFDM) and is considered to be a more competitive waveform in the future generation cellular communications. In current FBMC, the prototype filter is deliberately designed to meet the perfect reconstruction (PR) constraint to establish subband orthogonality in real domain, which may not be optimal from communication perspective. In this paper, we challenge the necessity of PR constraint by proposing a new FBMC framework, which directly accepts non-orthogonal transmission. The resulting imperfect reconstruction FBMC (iPR-FBMC) has several advantages over its PR FBMC counterpart: 1) the constraint on the prototype filter is relaxed; 2) more importantly, the prototype filter can now be optimized with new goal of improving the detection performance rather than having to meet the PR condition; and 3) it allows for more flexible subband management in multi-user scenario. We will show how those advantages can be exploited. Simulations show that with moderate increase in computational complexity, the proposed iPR-FBMC with optimized prototype filter has superior bit error rate (BER) performance to existing FBMC with PR constraint and even outperforms OFDM, especially in highly frequency selective channels. The findings may shed light into potential research on non-orthogonal FBMC without PR constraint.**

***Index Terms*— FBMC, OFDM, non-orthogonal transmission, prototype filter design, new waveforms.**

I. Introduction

ORTHOGONAL frequency division multiplexing (OFDM) is a successful waveform adopted in 4G network for its distinct advantages derived from its orthogonality of subcarriers. However, such orthogonality is achieved through sinc-shaped frequency response of subcarriers and requires stringent time and frequency synchronization. In addition, the usage of cyclic prefix (CP) also decreases its spectral efficiency. Therefore, new waveforms have been proposed to better cater the needs of future generation cellular communication systems, which include diverse communication scenarios that may require asynchronized transmission, low out-of-band radiation, and high spectral efficiency, where OFDM may not be the best choice. Among many candidates, filter bank multi-carrier (FBMC) is a promising one and can be viewed as a basis for many other new waveforms [1]–[3]. Different from OFDM, FBMC adopts a bank of frequency-well-localized filters, including synthesis filter bank (SFB) at the transmitter side and the analysis filter bank (AFB) at the receiver side, such that its non-adjacent subbands can be separated almost perfectly in frequency domain. Due to this property, FBMC is more robust to carrier frequency offset than OFDM. It also has lower out-of-band radiation and allows for totally asynchronized transmission. In addition, CP is not required in FBMC, which leads to higher spectral efficiency for long data packets [4].

Although FBMC entitles many inherent advantages over OFDM, it still shares a similar property as OFDM: it relies on subband orthogonality but in real-domain, i.e., in ideal channel, the real domain signal of a subband is orthogonal to that of other subbands. This orthogonality is established by carefully designing a real-valued low-pass prototype filter from which the synthesis and analysis filters of FBMC are derived. The condition of orthogonality is also widely referred to as perfect reconstruction (PR) or nearly perfect reconstruction (NPR) condition in literature,[1] depending on whether the orthogonality is perfectly or nearly perfectly met. Such a design strategy is originally proposed in audio and image signal processing rather than in the communication area. Although orthogonality is a good property as it allows for simple symbol detection especially in additive white Gaussian noise (AWGN) channel, it is not perfect from communication perspective. In practice, non-ideal factors such as channel distortion always destroy the orthogonality and complicated equalization techniques are needed to restore it. In addition, PR condition can be rather difficult to meet in some circumstances where non-uniform or even time-varying spectrum splitting is required. More importantly, the real domain orthogonality means the power on the imaginary part of the received signal may not be well utilized for symbol detection, otherwise deliberate receiver design must be involved. On the other hand, literature has proved that orthogonality

Manuscript received January 4, 2017; revised April 28, 2017; accepted May 26, 2017. Date of publication June 5, 2017; date of current version September 14, 2017. This work is supported by NSFC projects (61601119, 61571105, 61501109) and Jiangsu NSF project (No. BK20140646). The associate editor coordinating the review of this paper and approving it for publication was E. K. S. Au. *(Corresponding author: Zaichen Zhang.)*

J. Dang, Z. Zhang, and L. Wu are with the National Mobile Communications Research Laboratory, Southeast University, Nanjing 210096, China (e-mail: newwanda@seu.edu.cn; zczhang@seu.edu.cn; wuliang@seu.edu.cn).

Y. Wu was with the Institute for Communications Engineering, Technical University of Munich, D-80333 Munich, Germany. He is now with the Shanghai Key Laboratory of Navigation and Location Based Services, Shanghai Jiao Tong University, Minhang 200240, China (e-mail: yongpeng.wu2016@gmail.com).

Color versions of one or more of the figures in this paper are available online at http://ieeexplore.ieee.org.

Digital Object Identifier 10.1109/TCOMM.2017.2712178

[1]For simplicity and without confusion we will just use PR to refer to both PR and NPR throughout this paper.

in complex domain is impossible for critically sampled plain FBMC [5]. For those facts, one may ask, whether the orthogonality, either in real or complex domain, is really necessary for FBMC?

In this paper, we show the answer is no. A new framework of FBMC is proposed which simply drops the orthogonality constraint. Our paper basically proves that using non-orthogonal transmission in FBMC is indeed feasible and the signal is recoverable through simple signal processing algorithms with moderate complexity. We refer to this new framework of FBMC as imperfect reconstruction FBMC (iPR-FBMC) in the following. We will show that, the symbol detection is not only feasible but also has superior performance than current FBMC with PR constraint (PR-FBMC) and even outperforms OFDM, which is rarely found in literature. In addition, the new iPR-FBMC is capable of supporting more flexible subband allocation than PR-FBMC in multi-user communication, which shows potential gains by applying advanced resource management. Another new feature of iPR-FBMC is that its prototype filter can now be redesigned with the goal of improving the detection performance rather than having to meet the PR constraint, which leads to significant performance gains. In addition, new prototype filter design method for a smaller number of subbands is proposed to remedy the error floors incurred in previous design, which shows substantial improvement on the bit error rate (BER) performance.

Currently, only limited work is dedicated to this topic. In a recent review on FBMC, the authors questioned the optimality of using PR design in FBMC but leaves it as an open problem [6]. In fact, the feasibility of dropping PR condition has been shown in some works that adopt CP to the original FBMC. For example, [7] proposed to combine OFDM with FBMC, which does drop the orthogonality, but the symbol rate is halved as only half of the subbands are active for each data block, which essentially restores orthogonality in time domain. Recently an alternative CP based FBMC system has been proposed which achieves good performance with low complexity [8], [9]. However, CP is also used there which hinders the advantage of FBMC in spectral efficiency. In this paper, we take a further step and propose rigourously iPR-FBMC without CP at all. Other related issues include the rate analysis with utilized intrinsic interference [10] and the way of utilizing the intrinsic interference [11]–[13] in the framework of PR-FBMC. Those works revealed the potential gains of FBMC by exploiting the non-orthogonal part of the received signal, which further implies the potential of more general iPR-FBMC scheme.

This paper is organized as follows. Section II reviews existing PR-FBMC systems and proposes iPR-FBMC with detailed transceiver design. Section III gives performance analysis and comparison on the achievable rates, received signal-to-noise ratio (SNR) and computational complexities of different systems. Section IV introduces two different approaches for the optimization of the prototype filter. Multiple access issue is addressed in section V. Various simulations are given in section VI. Finally, section VII draws conclusions and sheds some light on future research.

Notation: Bold symbol $\mathbf{X}$ denotes a matrix. Bold and italic symbol $\boldsymbol{X}$ denotes a vector. Superscripts $(\cdot)^*$, $(\cdot)^{\mathcal{T}}$, and $(\cdot)^{\mathcal{H}}$ denote complex conjugate, transpose and Hermitian transpose, respectively. $\Re\{\cdot\}$ and $\Im\{\cdot\}$ denote taking the real and imaginary parts of a complex number, respectively. Normal symbol $*$ denotes linear convolution. $\mathcal{CN}(\boldsymbol{\mu}, \boldsymbol{\Sigma})$ denotes a circular Gaussian random vector with mean $\boldsymbol{\mu}$ and covariance matrix $\boldsymbol{\Sigma}$. $Q[x]$ denotes the hard decision of a modulated symbol. $\triangleq$ denotes definition. Function $\delta[n]$ equals to 1 for $n = 0$ and 0 otherwise. $\|\boldsymbol{X}\|$ denotes the ℓ^2-norm of a vector $\boldsymbol{X}$. $\det(\mathbf{X})$ denotes the determinant of matrix $\mathbf{X}$. $\Pr\{A\}$ is the probability of even A.

II. System Model

A. Existing PR-FBMC

In this subsection we provide a brief review of existing FBMC systems with PR constraint. The most popular system is typically referred to as OFDM/OQAM (OFDM with offset-QAM) [14]. Its basic idea is to convert the modulated (complex) QAM symbols to real PAM ones by taking, staggered in time, their real and imaginary parts. Those staggered pure real symbols are phase rotated and fed to the complex SFB with 2x oversampling, i.e., the upsampling factor P of the filter bank is only half of its total number of subbands, denoted by M. Since only real samples are processed by 2x oversampled filter banks, OFDM/OQAM is essentially *critically* sampled. Another critically sampled PR-FBMC system is exponentially modulated filter bank (EMFB) which directly maps the source bits to real PAM symbols before sending them to 2x oversampled SFB [15]. In [16], it has elaborated the relationship between EMFB and OFDM/OQAM. It is found that they share similar principles but EMFB has more efficient implementation and simpler mathematical tractability as it avoids the phase rotations in OFDM/OQAM. In this paper, we pick EMFB as a representative of PR-FBMC and a benchmark for comparison, whose system diagram is shown in Fig. 1. Therein, all the synthesis and analysis filters $f_m(l)$ and $h_m(l)$ are derived from a common lowpass prototype filter $\{h_p(l)\}_{l=0}^{N_f-1}$ of length N_f through frequency shifting [17]:

$$\begin{cases} f_m(l) = h_p(l)\exp\left(j\dfrac{2\pi}{M}\left(m-\dfrac{1}{2}\right)\left(l+\dfrac{M/2+1}{2}\right)\right), \\ h_m(l) = f_m^*(N_f-1-l), \end{cases} \quad (1)$$

for subband indices $m = 1, \ldots, M$, and filter tap indices $l = 0, 1, \ldots, N_f - 1$. $\{h_p(l)\}_{l=0}^{N_f-1}$ should be deliberately designed to meet the PR constraint. In this paper, we use the method in [18] to design $\{h_p(l)\}_{l=0}^{N_f-1}$ which gives fairly good performance. The filter response for $M = 16$ and $N_f = 64$ is illustrated in Fig. 2, which shows that the subband filters are well-localized and separated in frequency for nonadjacent ones. Without channel and noise, the PR constraint implies that in Fig. 1,

$$\Re\{y_m(n)\} = x_m(n-D), \quad \forall m, \quad (2)$$

where $\{x_m(n)\}_{n=0}^{\infty}$ are the real input PAM symbols to the m-th subband of SFB and D is some integer denoting time delay and

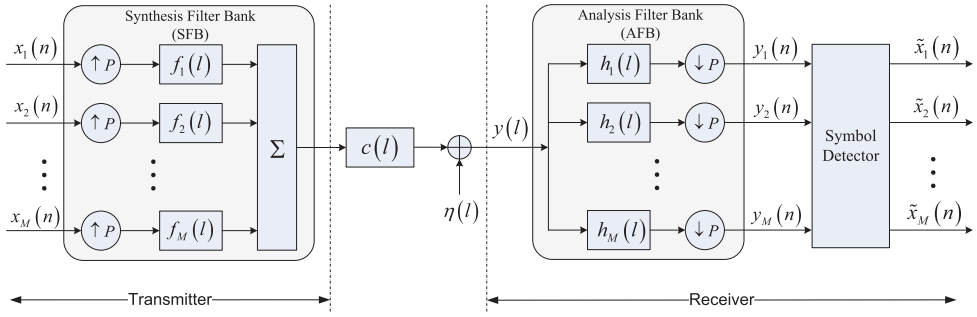

Fig. 1. Transceiver diagrams of existing PR-FBMC (EMFB) and proposed iPR-FBMC systems. For EMFB, $x_m(n)$ is PAM modulated and $P = M/2$; for iPR-FBMC, $x_m(n)$ is QAM modulated and $P = M$.

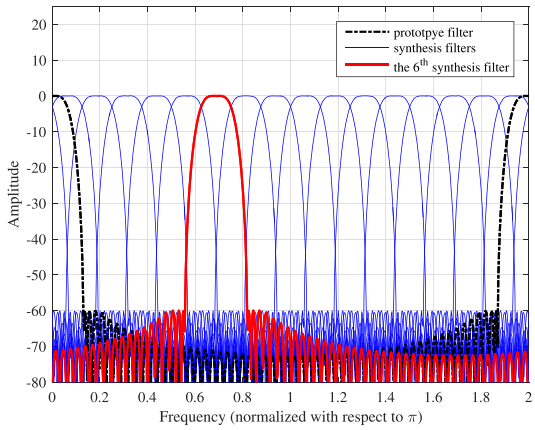

Fig. 2. Magnitude response of the prototype filter and synthesis subband filters for $M = 16$ and N_f=64.

is dependent on M and N_f. Eq. (2) indicates the orthogonality between different subbands in real domain (as the opposite side, $\Im\{y_m(n)\}$ is independent of $\{x_m(n)\}_{n=0}^{\infty}$ but is nonzero and relates to $\{x_{m-1}(n)\}_{n=0}^{\infty}$ and $\{x_{m+1}(n)\}_{n=0}^{\infty}$). A similar relationship also exists for OFDM/OQAM.

In frequency selective channels, the PR condition is destroyed and equalization is required to restore the orthogonality. A variety of equalization techniques, including single- and multi-tap equalization with and without cross-subband processing, have been investigated and compared with the performance of OFDM [19]. However, the BER performance is still not quite satisfactory and is generally lower bounded by that of OFDM.

B. System Model of iPR-FBMC

1) Transmitter Side: In this paper we propose a new framework of FBMC which does not rely on any subband orthogonality, neither in real nor complex domain. As Fig. 1 shows, our proposed iPR-FBMC system is derived from existing PR-FBMC but the input modulated symbols $\{x_m(n)\}_{n=0}^{\infty}$, $\forall m$, are selected to be standard complex QAM symbols without any fancy preprocessing. The complex symbols are directly processed by a SFB. The output of the SFB is transmitted through a multipath channel $\{c(l)\}_{l=0}^{L_c-1}$ of length L_c and corrupted by AWGN $\eta(l)$ that is distributed according to $\mathcal{CN}(0, N_0)$.

Here, the upsampling factor P in the SFB could be smaller than or equal to M. When $P = M$, the complex valued filter bank is critically sampled, which will be used in this paper for illustration purpose. However, the idea could be extended to the case of oversampled system, i.e., when $P < M$. All the synthesis filters can be exactly the same as that in PR-FBMC. However, since the input symbols are now complex ones, the real orthogonality between subbands does not hold any more even using the same filters. Therefore, theoretically, the prototype filter can now be chosen arbitrarily, as long as its frequency response is confined within a predefined spectrum mask, which greatly simplifies the design task of FBMC, especially in non-uniform or time-varying spectrum splitting scenarios. In fact, a more exciting advantage for the relaxed condition is that one can redesign the filters to directly improve the system performance without being bothered by the PR constraint. We will show how this new design freedom of the subband filters could be exploited in Section IV.

2) Receiver Side: At the receiver, an AFB is first employed to decompose the full band signal $\{y(l)\}_{l=0}^{\infty}$ into M subband signals $\{y_m(n)\}_{n=0}^{\infty}$, for $m = 1, 2, \ldots, M$. The analysis filters of the AFB are chosen based on the synthesis ones according to (1). The downsampling factor of the AFB is also chosen as $P = M$. Reference [5] has proved that such a straightforward filter bank structure can never meet the PR property, i.e., orthogonality in complex domain with critically sampling for such a filter bank structure is theoretically infeasible. Nonetheless, successful data decoding is still possible for this non-orthogonal iPR-FBMC with the aids of signal processing algorithms. This job is done by the symbol detector module after the AFB processing in Fig. 1.

Now we investigate the symbol detection algorithm that generates the symbol estimates $\{\{\tilde{x}_m(n)\}_{n=0}^{\infty}\}_{m=1}^{M}$ based on the observations of $\{\{y_m(n)\}_{n=0}^{\infty}\}_{m=1}^{M}$. In this paper, we assume the channel state information (CSI) is perfectly known at the receiver side. In general, there exists many candidate solutions for this problem. As a preliminary work, in this paper we propose to use per-subband linear minimum mean square error (MMSE) equalization with iterative interference cancellation, which is a natural choice since the decomposed signal of each subband is contaminated by limited interference that comes mainly from the adjacent subbands due to the fast attenuation of subband filters. The signal model can be established based on *polyphase identity* [20, Sec. 4.2], which

states that a cascade of interpolation (of factor M), linear filtering and decimation (of factor M) is equivalent to another linear filtering using the first polyphase component of the original filter. Therefore, the signal of subband-m after AFB can be written as

$$y_m(n) = g_{m,m}(n) * x_m(n) + I_m(n) + \eta_m(n), \quad (3)$$

$$I_m(n) \approx g_{m,m-1}(n) * x_{m-1}(n) + g_{m,m+1}(n) * x_{m+1}(n), \quad (4)$$

where $I_m(n)$ denotes the interference imposed on the interested signal of subband-m. Note that due to fast attenuation of the frequency response of subband filters, the interference perceived by subband-m comes mainly from its two neighbors, i.e., subbands $(m-1)$ and $(m+1)$. The filter $\{g_{m,j}(n)\}_{n=0}^{N_g-1}$ of length N_g is defined as the first polyphase component of the cascaded filter

$$v_{m,j}(l) \triangleq f_j(l) * c(l) * h_m(l), \quad (5)$$

i.e.,

$$g_{m,j}(n) \triangleq v_{m,j}(nM). \quad (6)$$

Note that $\{g_{m,j}(n)\}_{n=0}^{N_g-1}$ has much *shorter* length compared to that of $v_{m,j}(l)$. Finally, $\eta_m(n)$ is the filtered and downsampled noise. By normalizing the power of each analysis filter to unity, it is easy to show that $\eta_m(n) \sim \mathcal{CN}(0, N_0)$, $\forall m, n$.

The basic idea of symbol detection is to generate a specific linear MMSE equalizer of finite length for each subband. During the generation of an equalizer, the residual interference from mainly the adjacent subbands is not accounted for, which means we can use a same equalizer for all iterations. Although this is not optimal for signal estimation, it does not require the exact knowledge of the distribution of residual interference at each iteration and thus greatly simplifies the equalizer design. Simulations will show its effectiveness. At each iteration, the interference will be estimated and subtracted first before equalization. After several number of iterations, the performance will converge to a certain level and hard decision could be made. The procedure is stated in Algorithm 1.

Note that the similar idea has been investigated in [21] for PR-FBMC, but therein the equalizer is designed based on multi-subbands, which is more complex and needs to be regenerated at every iteration. Our proposed symbol detection algorithm is much simpler. As will be shown in VI, it is quite effective and the BER performance even outperforms that of OFDM.

Algorithm 1 Symbol Detection Algorithm for iPR-FBMC

Input: $\{g_{m,j}(n)\}_{n=0}^{N_g-1}$, $m, j = 1, 2, \ldots, M$, N_0 and T, the total number of iterations.

Initialization:

i) Generate a set of M linear MMSE equalizers, denoted by $\{w_m(n)\}_{n=0}^{L_w-1}$ for each $m = 1, 2, \ldots, M$, respectively;

ii) Set hard decisions $\tilde{x}_m(n) = 0$, $\forall\, m, n$;

iii) Set $t \leftarrow 1$.

Iterative processing:

While $t \le T$ **do**

For every m, $m = 1, 2, \ldots, M$, **do**

1) Interference estimation:

$$\tilde{I}_m(n) = g_{m,m-1}(n) * \tilde{x}_{m-1}(n) + g_{m,m+1}(n) * \tilde{x}_{m+1}(n);$$

2) Interference cancellation:

$$\check{y}_m(n) = y_m(n) - \tilde{I}_m(n);$$

3) Equalization:

$$\hat{x}_m(n) = w_m(n) * \check{y}_m(n);$$

4) Hard decision:

$$\tilde{x}_m(n) = Q[\hat{x}_m(n)].$$

end for

$t \leftarrow t + 1$.

end while

Output: $\{\tilde{x}_m(n)\}$, $\forall\, m, n$.

III. Performance Analysis

A. Achievable Rate

In this subsection, we compute and compare the achievable rate of iPR-FBMC with that of PR-FBMC and OFDM. Based on Fig. 1, we will compute the achievable rate by observing the aggregate signal $\{y(l)\}_{l=0}^{\infty}$ before AFB rather than observing the subband signals $\{\{y_m(n)\}_{n=1}^{\infty}\}_{m=1}^{M}$. The reason is explained as follows. The AFB module is *nothing* but a part of a receiver without any known optimality. From information theory, the mutual information between the source symbols $\{\{x_m(n)\}_{n=0}^{\infty}\}_{m=1}^{M}$ and processed symbols $\{\{y_m(n)\}_{n=0}^{\infty}\}_{m=1}^{M}$ is no larger than that of between $\{\{x_m(n)\}_{n=0}^{\infty}\}_{m=1}^{M}$ and immediate received symbols $\{y(l)\}_{l=0}^{\infty}$. Therefore, choosing $\{y(l)\}_{l=0}^{\infty}$ to compute the achievable rate will expose the greatest potential of iPR-FBMC. In other words, although AFB is utilized so far in literature and in this paper, we cannot rule out the possible receiver structure that does not use AFB processing at all. Interestingly, observing $\{y(l)\}_{l=0}^{\infty}$ is equivalent to observing $\{\{y_m(n)\}_{n=0}^{\infty}\}_{m=1}^{M}$ if the analysis filters $h_m(l)$ are chosen as delay chains of length M:

$$h_m(l) = \delta[l - m + 1], \quad l = 0, 1, \ldots, M-1, \ \forall m. \quad (7)$$

Therefore, without confusion, we will still use $\{\{y_m(n)\}_{n=0}^{\infty}\}_{m=1}^{M}$ in this section for rate analysis but the corresponding analysis filters are redefined by (7).

1) AWGN Channel: Firstly, we consider transmission in AWGN channel. Now, using polyphase identity again, the received signal is given by

$$y_m(n) = \sum_{j=1}^{M} g_{m,j}(n) * x_j(n) + z_m(n), \quad (8)$$

where $z_m(n)$ is the m-th polyphase component of the original noise $\eta(l)$. Different from (3), $y_m(n)$ in (8) is of *full band* and contains M nonnegligible signal components. In addition, the noise $z_m(n)$ is now unfiltered and i.i.d Gaussian with zero mean and variance N_0. Analogous to the technique used in [22, Sec. 5.3.3] for calculating the capacity of a frequency selective channel, we assume N_d independent subcarriers

are utilized to transmit N_d modulated symbols per subband, by adding a cyclic prefix of length $N_g - 1$. And this operation is repeated over blocks of data symbols. Then, for each data block, the frequency domain received signal on subband-m is given by

$$Y_m(q) = \sum_{j=1}^{M} G_{m,j}(q) X_j(q) + Z_m(q), \tag{9}$$

where $\{Y_m(q)\}_{q=0}^{N_d-1}$, $\{X_j(q)\}_{q=0}^{N_d-1}$, $\{Z_m(q)\}_{q=0}^{N_d-1}$ and $\{G_{m,j}(q)\}_{q=0}^{N_d-1}$ are the N_d-point DFT of $\{y_m(n)\}_{n=0}^{N_d-1}$, $\{x_j(n)\}_{n=0}^{N_d-1}$, $\{z_m(n)\}_{n=0}^{N_d-1}$ and $\{g_{m,j}(n)\}_{n=0}^{N_g-1}$, respectively. Collecting all the subband signals for a same q, one gets

$$\boldsymbol{Y}(q) = \mathbf{G}(q)\boldsymbol{X}(q) + \boldsymbol{Z}(q), q = 0, 1, \ldots, N_d - 1, \tag{10}$$

where $\boldsymbol{Y}(q) = [Y_1(q), Y_2(q), \ldots, Y_M(q)]^{\mathcal{T}}$, $\boldsymbol{X}(q) = [X_1(q), X_2(q), \ldots, X_M(q)]^{\mathcal{T}}$, $\boldsymbol{Z}(q) = [Z_1(q), Z_2(q), \ldots, Z_M(q)]^{\mathcal{T}}$ and the (m, j)-th entry of the $M \times M$ matrix $\mathbf{G}(q)$ is given by $G_{m,j}(q)$. Collecting all $\boldsymbol{Y}(q)$ in a column, we get the matrix form

$$\boldsymbol{Y} = \mathbf{G}\boldsymbol{X} + \boldsymbol{Z}, \tag{11}$$

where $\boldsymbol{Y} = [\boldsymbol{Y}(0), \boldsymbol{Y}(1), \ldots, \boldsymbol{Y}(N_d - 1)]^{\mathcal{T}}$, $\boldsymbol{X} = [\boldsymbol{X}(0), \boldsymbol{X}(1), \ldots, \boldsymbol{X}(N_d - 1)]^{\mathcal{T}}$, $\boldsymbol{Z} = [\boldsymbol{Z}(0), \boldsymbol{Z}(1), \ldots, \boldsymbol{Z}(N_d - 1)]^{\mathcal{T}}$, and $\mathbf{G}$ is a block diagonal matrix whose diagonal elements are $\mathbf{G}(q)$, $q = 0, 1, \ldots, N_d - 1$. Eq. (11) is a multiple input multiple output (MIMO) model whose maximum rate is achieved by transmitting on the eigenchannels of $\mathbf{G}$ with proper powers [22, Sec. 7.1.1]. Denote the singular value decomposition (SVD) of $\mathbf{G}$ by

$$\mathbf{G} = \mathbf{U}\mathbf{S}\mathbf{V}^{\mathcal{H}}, \tag{12}$$

where $\mathbf{S}$ is a diagonal matrix whose diagonal elements are the singular values $\mu(k)$ in descending order, $k = 0, 1, \ldots, MN_d - 1$, and $\mathbf{U}$, $\mathbf{V}$ are unitary matrices. Assuming there are M_p positive singular values and the power allocated to the k-th eigenchannel of $\mathbf{G}$ is $P(k)$, the optimal transmission is given by

$$\boldsymbol{Y} = \mathbf{G}\mathbf{V}\tilde{\boldsymbol{X}} + \boldsymbol{Z}, \tag{13}$$

where the power of $\tilde{X}(k)$ is given by $P(k)$ for $k < M_p$ and 0 otherwise. The maximum achievable rate is obtained by solving problem **(P1)**:

$$\max_{\{P(k)\}} R = \frac{1}{MN_d} \sum_{q=0}^{M_p-1} \log_2\left(1 + \frac{P(k)\mu^2(k)}{N_0}\right)$$
$$\text{s.t.} \begin{cases} \dfrac{1}{MN_d} \displaystyle\sum_{k=0}^{M_p-1} P(k)\mu^2(k) = P_x \\ P(k) \geq 0, \quad \forall k \end{cases} \tag{P1}$$

where P_x is the average transmitted power. Note that the first constraint is different from that in the conventional MIMO model. It essentially says that the average power of the *transmitted* signal $\mathbf{G}\mathbf{V}\tilde{\boldsymbol{X}}$ in (11) rather than $\mathbf{V}\tilde{\boldsymbol{X}}$ is P_x. It can be easily shown that the optimal solution of **(P1)** is given by

$$P_{opt}(k) = \frac{MN_d P_x}{M_p \mu^2(k)}, \quad k = 0, 1, \ldots, M_p - 1, \tag{14}$$

and the maximal achievable rate is given by

$$R = \frac{M_p}{MN_d} \log_2\left(1 + \frac{MN_d}{M_p}\frac{P_x}{N_0}\right). \tag{15}$$

From (15), we find that the rate is closely related to M_p, the number of nonzero singular values of $\mathbf{G}$, which is determined by the prototype filter. This implies the potential of designing optimal prototype filter to maximize the achievable rate.

2) Frequency Selective Channel: For frequency selective channel, we assume the CSI is perfectly known at the receiver but the transmitter does not know it. With this assumption, the transmitter has to process the signal as if in AWGN channel, i.e., allocate powers and transmit on the eigenchannels of $\mathbf{G}$ with positive eigenvalues. The achievable rate $R(\boldsymbol{c})$ given a specific channel $\boldsymbol{c} = \{c(l)\}_{l=0}^{L_c-1}$ could be readily calculated by [22, Sec. 8.2.1]:

$$R(\boldsymbol{c}) = \frac{1}{MN_d} \log_2 \det\left(\mathbf{I} + \frac{1}{N_0}\mathbf{G}_{\boldsymbol{c}}\mathbf{V}\Lambda\mathbf{V}^{\mathcal{H}}\mathbf{G}_{\boldsymbol{c}}^{\mathcal{H}}\right), \tag{16}$$

in which Λ denotes a diagonal matrix whose k-th main diagonal entry is $P_{opt}(k)$ that are obtained in AWGN channel (c.f. (14)), $\mathbf{G}_{\boldsymbol{c}}$ is defined similarly to $\mathbf{G}$ in (11) by replacing $f_j(l)$ with $f_j(l) * c(l)$, i.e., the instantaneous channel is taken into consideration, and $\mathbf{V}$ is defined in (12) in AWGN channel. Then, the average rate over many realizations of channels is given by

$$R = \mathrm{E}\{R(\boldsymbol{c})\}, \tag{17}$$

where the expectation $\mathrm{E}\{\cdot\}$ is taken with respect to the stationary distribution of the channel state.

3) Comparison With PR-FBMC and OFDM: For PR-FBMC, similar approach could be employed to compute its rate. The key differences include: i) the factor of upsampling and downsampling changes to $M/2$; ii) the input symbols are real. For OFDM, equal power allocation among subcarriers is optimal for AWGN channel. In frequency selective channel, when the transmitter does not have CSI, equal power should be still used and the average rate is calculated by finding the mean value of rates over many OFDM symbols with random channel realizations.

Fig. 3 shows the achievable rates of single user iPR-FBMC, OFDM and PR-FBMC with different number of subbands/subcarriers M. The rates are also compared with that of channel capacity in both AWGN and frequency selective channels. For the latter, the channel is modeled as a L_c-tap complex random Gaussian channel with equal power gains among the taps and the total power is normalized to unity. Here $L_c = 16$. It can be seen that in AWGN channel, all schemes are capacity achieving regardless of M. However, in frequency selective channel, only iPR-FBMC and PR-FBMC are capacity achieving and OFDM is not for small M. This is not surprising. The channel capacity is obtained by using the same approach as

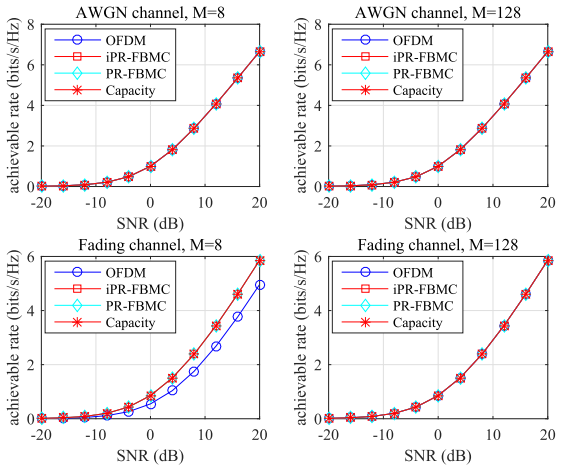

Fig. 3. Achievable rate comparison of OFDM, iPR-FBMC, PR-FBMC and channel capacity.

OFDM but with infinite number of subcarriers such that every point of frequency response is considered for transmitting data. On the other hand, OFDM with small M only captures part of the channel state information through limited number of isolated frequency points, leading to loss of information of the channel. For iPR-FBMC and PR-FBMC, they can cover all channel response through overlapped subband filtering and the transmission does not only rely on M specific frequency points. Therefore, through power allocation and proper signal rotation (by $\mathbf{V}$, c.f. (16)), they can achieve the capacity for any M.

Finally, we note that in Fig. 3 and all the figures in the rest of this paper, the power/spectral efficiency penalty caused by the overhead of CP in OFDM and the tailing in FBMC are *not* accounted for in calculations.

B. Received SNR Analysis

In this subsection, we compare the received SNR of iPR-FBMC and OFDM in frequency selective channel and show that iPR-FBMC is more robust to channel deep fading. Consider the first subcarrier/subband. For OFDM, the received SNR of this subcarrier is given by

$$J_o = \frac{P_x |H(e^{j\omega})|^2_{\omega=0}}{N_0} = |H(e^{j\omega})|^2_{\omega=0}\text{SNR}, \tag{18}$$

where $\text{SNR} \triangleq P_x/N_0$ is defined as the transmitted SNR and $H(e^{j\omega})$ is the frequency response of channel $\boldsymbol{c} = [c(0), c(1), \ldots, c(L_c-1)]^{\mathcal{H}}$. It can be easily shown that

$$J_o = \text{SNR} \sum_{l_1=0}^{L_c-1} \sum_{l_2=0}^{L_c-1} c(l_1)c^*(l_2) = \boldsymbol{c}^{\mathcal{H}}\mathbf{T}_o\boldsymbol{c}, \tag{19}$$

where $\mathbf{T}_o$ is an $L_c \times L_c$ matrix whose entries are all 1. As $c(l)$ are circular Gaussian, J_o is a generalized chi-squared distributed random variable.

For iPR-FBMC, the original signal is transmitted through the synthesis and analysis filters whose frequency responses are confined within the range $[-\frac{\pi}{M}, \frac{3\pi}{M}]$, as illustrated by Fig. 2. In AWGN channel, the received power is given by $P_x \sum_{n=0}^{N_g-1} |g_{1,1}(n)|^2$. In practice, the filters are normalized such that $\sum_{n=0}^{N_g-1} |g_{m,m}(n)|^2 = 1$ to avoid any amplitude amplification in AWGN channel. In frequency selective channel, due to the spectrum confinement of subband filters, the transmitted subband signal, whose power spectral density is flat, is only affected by the channel response in the same frequency range $[-\frac{\pi}{M}, \frac{3\pi}{M}]$ when passing through the channel. Since linear convolution with channel in time domain can be interpreted as product in frequency domain, the received SNR can be written as

$$\begin{aligned} J_F &= \text{SNR} \cdot \frac{M}{4\pi} \int_{-\frac{\pi}{M}}^{\frac{3\pi}{M}} |H(e^{j\omega})|^2 d\omega \\ &= \text{SNR} \cdot \frac{M}{4\pi} \int_{-\frac{\pi}{M}}^{\frac{3\pi}{M}} \left| \sum_{l=0}^{L_c-1} c(l) e^{-jl\omega} \right|^2 d\omega \\ &= \text{SNR} \cdot \boldsymbol{c}^{\mathcal{H}}\mathbf{T}_F\boldsymbol{c}, \end{aligned} \tag{20}$$

where $\mathbf{T}_F$ is a Hermitian matrix of size $L_c \times L_c$ whose elements are given by $\mathrm{T}_F(l_1, l_2) = \text{sinc}\left[\frac{2}{M}(l_1 - l_2)\right] e^{j\frac{\pi}{M}(l_1-l_2)}$. Therefore, J_F is also a generalized chi-squared random variable. Note that here J_F does not consider the interference of the neighbouring subbands but exposes the fundamental behaviour of iPR-FBMC. Now we have the following observations:

1) $\mathrm{E}\{J_o\} = \mathrm{E}\{J_F\} = \text{SNR}$;

2) $J_F = J_o$ when any of the following conditions is met: i) $M \to \infty$; ii) $H(e^{j\omega})$ is a constant over the bandwidth of the corresponding subband filter;

3) Without the conditions of i) and ii), $\Pr\{J_F < \delta\} < \Pr\{J_o < \delta\}$, where δ is a small positive number.

The proofs of observations 1) and 2) are straightforward. The proof of observation 3) is listed in the Appendix. Observations 1) and 2) show the similarities of the two random received SNRs: they are *equal* in the average sense and becomes *identical* whenever the channel response within the subband becomes flat. Observation 3) unveils their difference: compared to OFDM, iPR-FBMC is less likely to incur a deep fading event, which can be defined as that the received SNR drops below a very small threshold. The intuition is that iPR-FBMC collects all the power of channel within the subband bandwidth such that the received power is more stable even there are frequency response variations. Therefore, iPR-FBMC is expected to have improved detection performance especially in highly frequency selective channels.

C. Detection Complexity

In this section we analyze the complexity of the proposed iPR-FBMC using order notation. The SFB and AFB parts have very efficient implementations using polyphase network and pipelined structure and the complexity could be comparable with that of OFDM [23], [24]. Here we focus on the complexity of the proposed symbol detection algorithm. Its computation burden consists of three parts: generation of MMSE equalizers, interference estimation and equalization.

1) Generation of Equalizers: This involves a matrix inversion operation, whose complexity is in the order of $O(L_w^3)$,

where L_w is the length of equalizer $w_m(n)$. For simplicity, we assume $L_w = \alpha N_g$. Therefore, the total complexity is in the order of $O(M\alpha^3 N_g^3)$ for all subbands. In general, $\alpha \geq 1$, however, for FBMC, $\{g_{m,m}(n)\}_{n=0}^{N_g-1}$ contains many zeros at the start and end of it, i.e., the *effective* length of $\{g_{m,m}(n)\}$ is much smaller than N_g. When M is getting larger, α is getting smaller. In addition, the complexity is independent of the amount of input symbols and the number of iterations T.

2) Interference Estimation: This involves convolution of signal with $g_{m,m\pm1}(n)$, which has complexity of $O(MN_dN_gT)$ in total, where N_d is the number of input symbols per subband.

3) Equalization: This involves convolution of signal with $w_m(n)$, which has complexity of $O(MN_d\alpha N_gT)$ in total.

In summary, the decoding complexity per QAM symbol is in the order of $O(\alpha^3 N_g^3/N_d)$ for equalizer generation and $O(N_gT)$ for signal estimation and equalization. The former diminishes for large N_d and the latter remains constant and is a bottleneck. This is more computation demanding compared to OFDM equalization of complexity $O(1)$. Fortunately, efficient algorithms for linear convolution have been investigated which performed computation in transform domain using fast implementation methods. For example, FFT and discrete cosine transform have been studied to reduce the complexity of convolution [25], [26]. The complexity could be reduced to $O(T\log_2 N_t)$ per symbol for iPR-FBMC signal estimation and equalization using FFT based algorithm, where N_t is the FFT size after sequence truncation. By selecting $N_t < 2^{N_g}$, the complexity could be reduced. In fact, FFT based fast convolution is also used to implement the SFB and AFB [27], which results in even lower complexity than that of the polyphase network implementation. Note that in practice, OFDM also needs additional complicated processing for time and frequency synchronization while FBMC may not need.

IV. Prototype Filter Optimization

So far, we have established the iPR-FBMC system based on current PR-FBMC with the same subband filters. As aforementioned, the PR constraint is not required any more and now we have new design freedom on the subband filters: we can adjust the filter coefficients to improve performance rather than to meet the PR constraint. In this section, we investigate efficient filter optimization methods to enhance the detection performance.

Firstly, we propose a universally feasible method for iPR-FBMC with different M. The idea is based on the observation that existing PR-FBMC decoding relies on the first polyphase component, i.e., $g_{m,m}(n) = v_{m,m}(nM)$, for each subband and the remaining $(M-1)$ polyphase components (denoted by $g_{m,m}^{(i)}(n) = v_{m,m}(nM+i-1)$ for $i = 2,\ldots,M$) are discarded. Although the remaining polyphase components are highly correlated with the first one and never meet the PR constraint (thus PR-FBMC only uses the first component), their average powers are not constant and even larger than the first one, which can now be exploited in the iPR-FBMC framework. Fig. 4 shows the power profiles of the polyphase components of a specific subband for $M = 16$ and $N_f = 64$ in both AWGN channel and a random realization

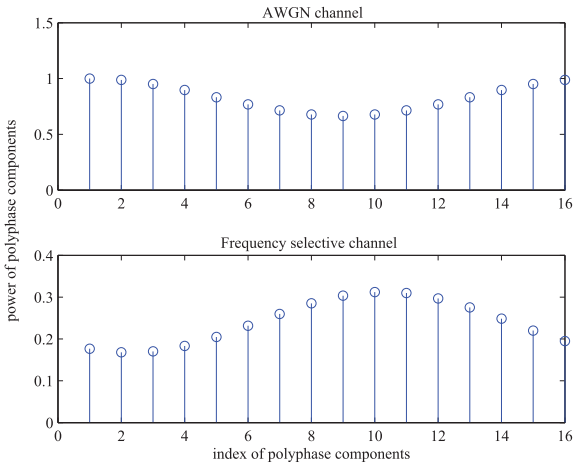

Fig. 4. Sample view of the power profiles of the polyphase components in AWGN and frequency selective channels.

of a 6-tap multipath channel (equal average power per tap). As it shows, in AWGN channel, the first polyphase components indeed has the largest power. However, in frequency selective channel, this result does not hold and other polyphase components may entitle larger power, e.g., the power of the tenth polyphase component is almost twice that of the first one.

Therefore, we will select the polyphase component with largest received power to enhance the detection performance. This is equivalent to adjust $h_m(l)$ in (1) by inserting some additional zeros at the beginning of it, which is a subband-specific redesign of the analysis filters. The effectiveness of this selection method will be verified by simulations.

Secondly, through simulations, we find that for small M, both PR-FBMC and iPR-FBMC incur error floors in highly frequency selective channels. To address this challenge, we also developed a new prototype filter design method for iPR-FBMC with small M. The basic idea is as follows: the main reason for an error floor event is that the first round iteration does not give fairly accurate estimations due to the relatively heavier overlapping of adjacent subbands with small M. Therefore, if one can improve the signal-to-interference-plus-noise ratio (SINR) at the first iteration, improved detection performance is expected after further iterations. Thus, analogous to [18], we adjust the cutoff frequency of $h_p(l)$ with a new goal of obtaining a better SINR rather than meeting the PR constraint. However, SINR will be overly maximized if the filter response is very narrow such that there is no overlapping between adjacent subbands. As the bandwidth is very limited in such a case, the performance is rather poor. To avoid this trivial design, we choose an approximation of the rate of a subband as the objective function, which combines the SINR and bandwidth:

$$r_m = B_m \log_2(1+\gamma_m), \tag{21}$$

where B_m is the 3-dB bandwidth of the response of $\{g_{m,m}(n)\}_{n=0}^{N_g-1}$, γ_m is the SINR of the received subband signal $y_m(n)$ and is defined by

$$\gamma_m = \frac{P_x\|\boldsymbol{g}_{m,m}\|^2}{P_x\|\boldsymbol{g}_{m,m-1}\|^2 + P_x\|\boldsymbol{g}_{m,m+1}\|^2 + N_0\|\boldsymbol{h}_m\|^2}, \tag{22}$$

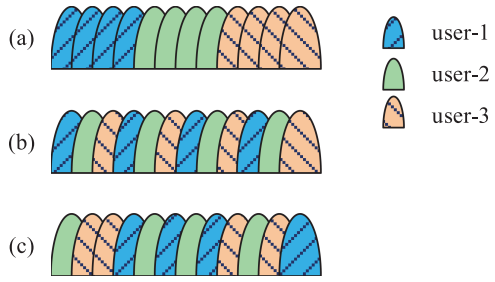

Fig. 5. Illustration of different subband allocation schemes for multiuser iPR-FBMC with 3 users and 12 subbands: (a) localized; (b) interleaved; (c) random.

where $\boldsymbol{g}_{m,k}$ is the vector form of $\{g_{m,k}(n)\}_{n=0}^{N_g-1}$ and $\boldsymbol{h}_m$ is the vector form of $\{h_m(l)\}_{l=0}^{N_f-1}$. Note that $\boldsymbol{g}_{m,k}$ $(k = m-1, m, m+1)$ is obtained in AWGN channel, i.e., the transmitter has no access to CSI, therefore, we only need to maximize r_m for a randomly chosen m to find the optimal $h_p(l)$. Simulations will show that the new design based on (22) gives substantial performance improvement.

V. Multiple Access Using iPR-FBMC

In multi-user communications, every subband of FBMC is exclusively allocated to a specific user for access. Analogous to orthogonal frequency division multiple access (OFDMA), there may exist three typical subband allocation schemes, i.e., localized, interleaved and random allocation, as shown in Fig. 5. In downlink, since each user sees a single channel from base station, the received signal model is essentially the same as the single-user case and all the three subband allocation schemes could be employed. However, there remains a major difference between PR-FBMC and iPR-FBMC in *uplink* transmission.

For PR-FBMC, suppose subband-k and its adjacent subband-$(k+1)$ is allocated to user-1 and user-2 respectively. Unless user-1 and user-2 transmit in a same channel, at the base station, equalization of subband-k's signal will not be perfect: the orthogonality could not be perfectly restored due to the overlapping of subband-$(k+1)$'s signal with a different channel response. Thus it is required that different users should be perfectly separated in frequency, which could be realized by inserting a null subband between users for isolation. As a consequence, only *localized* subband allocation scheme is practical for PR-FBMC in uplink. Interleaved and random subband allocation schemes are not suitable since they require excessive number (more than the number of users) of null subbands for isolation. This inevitably decreases the flexibility of system design.

For our proposed iPR-FBMC system, multiple access in uplink could be well-supported: the interference between subbands is artificially *allowed* and there is no need to use null subbands for isolation any more. Therefore, besides localized subband allocation, interleaved and random subband allocation schemes could also be used for multi-user iPR-FBMC in uplink without any null subbands. As a result, compared to PR-FBMC, not only the spectral efficiency could be improved by eliminating null subbands, but also the flexibility of the resource management could be improved. As will be seen in Section VI, by using interleaved subband allocation scheme, the frequency diversity collection capability could be improved compared to localized subband allocation.

TABLE I
Simulation Parameters of PR-FBMC, iPR-FBMC and OFDM

System Parameters	Possible Values
Modulation Formats	iPR-FBMC/OFDM: QPSK; PR-FBMC: BPSK
Data block length N_d	iPR-FBMC/OFDM: 100; PR-FBMC: 200
Number of subband/subcarriers M	$8, 128$
Length of subband filters for FBMC	$N_f = 6M$
Maximum passband/stopband deviations	0.001
Error ratio [18, Eq. (12)]	$\kappa = 1$
Length of equalizers for iPR-FBMC	$N_e = 2N_g$
Number of iterations for iPR-FBMC	$T = 6$
Length of multipath channels L_c	$3, 12$

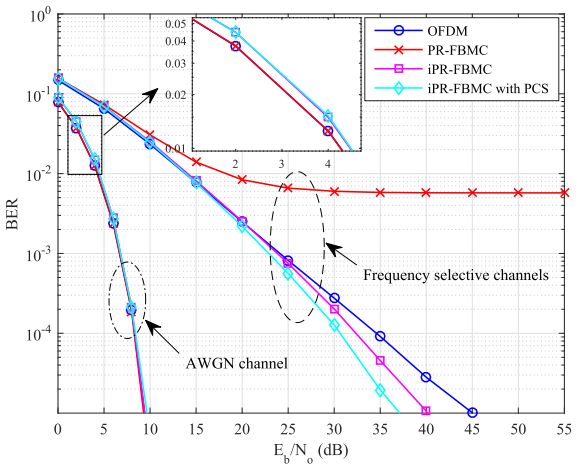

Fig. 6. BER comparison between OFDM, PR-FBMC and iPR-FBMC in both AWGN channel and frequency selective channel for $M = 128$ and $L_c = 12$.

VI. Simulations

In this section, we evaluate the BER performance of our proposed iPR-FBMC system and compare it with other benchmarks including PR-FBMC (EMFB) and OFDM. To make the comparison fair and clear, some key system parameters are defined in Table I. Other related configurations are defined here. The multipath channel is realized for 1000 times. To equalize, both PR-FBMC and OFDM employ typical single-tap subband/subcarrier MMSE equalizers. Channel coding is not involved in simulations. The power and spectral efficiency penalty caused by CP in OFDM and tailing of filters in FBMC is not accounted for in simulations. Finally, the legend 'iPR-FBMC' means proposed iPR-FBMC system using the same filters as PR-FBMC. The abbreviation 'PCS' in the legend for iPR-FBMC refers to optimized filter design using polyphase component selection. The abbreviation 'RM' in the legend for iPR-FBMC refers to optimized filter design using rate maximization based on (22).

A. BER of Point-to-Point Communication

First we simulate the BER in single user case. Fig. 6 shows the performance for $M = 128$. Both AWGN and frequency

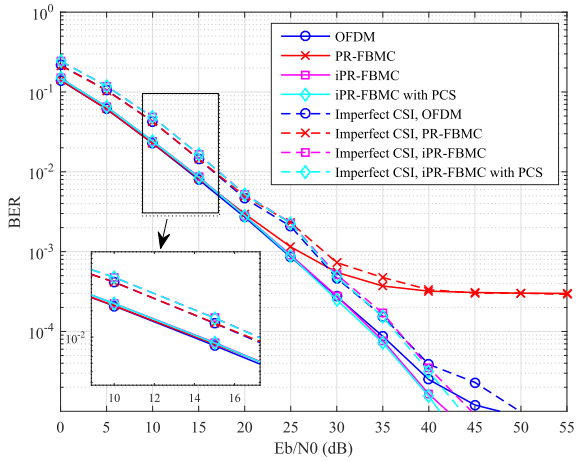

Fig. 7. BER comparison between OFDM, PR-FBMC and iPR-FBMC in frequency selective channel with channel estimation errors for $M = 128$ and $L_c = 3$.

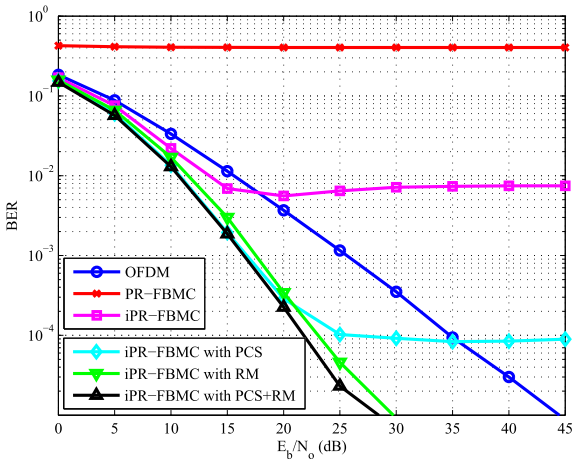

Fig. 8. BER comparison between OFDM, PR-FBMC and iPR-FBMC in frequency selective channels with $L_c = 12$ and $M = 8$.

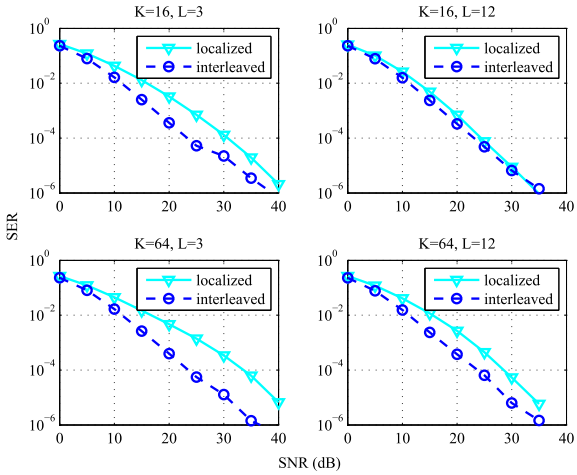

Fig. 9. SER of iPR-FBMC using localized and interleaved subband allocation schemes with $M = 128$ subbands in total.

selective channel of $L_c = 12$ are tested. In AWGN channel, the performance of PR-FBMC is the same as OFDM. The performance of iPR-FBMC (with or without PCS) is slightly worse. This is caused by potential error propagation in the procedure of iterative interference estimation and cancellation. Therefore, this effect is more pronounced in lower SNR range, as shown by Fig. 6. In frequency selective channels, the proposed iPR-FBMC outperforms conventional PR-FBMC whose BER incurs relatively high level error floor. In addition, iPR-FBMC even outperforms OFDM, especially in high SNR range. This is due to the fact that iPR-FBMC is able to collect all the power of a subband to combat the channel distortion but OFDM only depends on the center frequency point of a subcarrier. Therefore, compared to OFDM, iPR-FBMC is more robust to deep fading, which is the main impairment of a frequency selective channel. This is in accordance with the SNR analysis in Section III-B. Another observation from Fig. 6 is that for iPR-FBMC, selecting optimal polyphase component clearly enhances the detection performance. This verifies that in iPR-FBMC the filters could be redesigned to improve receiver performance rather than to just meet PR condition.

Fig. 7 shows effect of imperfect CSI on the BER performance in multipath channel with $L_c = 3$. For imperfect channel estimation, we employ the channel estimation model in [28] where the l-th estimated channel tap can be modeled by $\hat{c}(l) = \frac{1}{\rho}c(l) - \sqrt{1-\rho^2}v$, where v is a standard circular Gaussian random variable and ρ is related to SNR by $\rho = 1 - \frac{\text{SNR}}{2}$. In our simulation, we choose the relationship between MSE and SNR in dB scales as $(\text{MSE})_{\text{dB}} = -(\text{SNR})_{\text{dB}} - 15$. With this configuration, we obtain Fig. 7. It can be seen that with imperfect channel estimation, the BER performance is getting worse for all systems. However, due to the potential error propagation in the iterative processing of iPR-FBMC receiver, it tends to be more sensitive to channel estimation error compared to OFDM, as can be seen clearly in low SNR range. Nonetheless, the performance gap is limited and at high SNR range, iPR-FBMC still outperforms both OFDM and PR-FBMC with imperfect CSI.

Fig. 8 depicts the BER performance of different approaches with a small subband/subcarrier number $M = 8$ in a 12-tap frequency selective channel model. It can be seen that PR-FBMC and the original iPR-FBMC incur high error floors. Optimized iPR-FBMC with polyphase component selection improves the performance a lot but still suffers from error floor at high SNR regime. On the other hand, by using the prototype filter optimized through rate maximization, the BER could be improved significantly without error floor. Combined with polyphase component selection, the performance could be even better. This simulation result clearly shows the potential gain of using proposed iPR-FBMC with optimized filter design. Note that rate maximization method in its current formulation is only effective for small number of subbands. For large number of subbands, the residual interference is not dominating after sufficient number of iterations, therefore, maximizing the SINR of the first iteration does not necessarily lead to better performance after convergence.

B. Multiuser Communication With Different Subband Allocation Schemes

In this section, we compare two subband allocation schemes for multiuser iPR-FBMC with polyphase component selection:

one is localized allocation as previous simulations, and the other is interleaved allocation. To compare the frequency diversity collecting capability, the modulated symbols are repeated twice and spread to different subcarriers. We assume there are $K = 16$ and 64 users in total and simulate the symbol error rate (SER) performance in frequency selective channels with different length of channels. Fig. 9 shows the SER performance. It can be seen that by using interleaved subband allocation, the performance could be improved compared to localized subband allocation scheme, especially when the channel frequency selectivity is not quite severe. This clearly shows that interleaved subband allocation scheme is more capable of collecting multipath diversity gain than localized allocation, which is inline with intuition. This is a new feature that PR-FBMC does not entitle.

VII. Conclusions

This paper proposed an iPR-FBMC framework which drops the PR constraint in current FBMC systems. It allows for direct filtering of complex symbols and is more flexible in utilizing the subbands in multiuser scenario. Through advanced signal processing and filter optimization, its BER performance is superior to both OFDM and PR-FBMC systems. As a preliminary work, there remains many research challenges to complete this framework, such as rate analysis in multi-user communication (which will ultimately show the non-orthogonality nature of iPR-FBMC), more powerful signal processing using turbo receiver, universally optimal prototype filter design, combination with MIMO (which is expected to be easier compared to PR-FBMC), as well as channel estimation and resource allocation, which will be left for future study.

Appendix

Proof of observation 3): Denote $f_o(x)$ and $f_F(x)$ as the probability density functions (PDF) of J_o and J_F, respectively. They have definitions only for $x \geq 0$. To prove $\Pr\{J_F < \delta\} < \Pr\{J_o < \delta\}$ for a small number δ, $\delta > 0$, it is sufficient to show $f_F(x) < f_o(x)$ for $x < \delta$. Next, we investigate the relationship between $f_F(x)$ and $f_o(x)$ for small x. We perform eigen-decomposition of $\mathbf{T}_F$ as

$$\mathbf{T}_F = \mathbf{P}_F^{\mathcal{H}} \Lambda_F \mathbf{P}_F, \tag{23}$$

where Λ_F is a diagonal matrix whose entries on the main diagonal are the eigenvalues of $\mathbf{T}_F$. Since $\mathbf{T}_F$ is Hermitian, $\mathbf{P}_F$ is unitary and the eigenvalues of $\mathbf{T}_F$ is real. In addition, as $J_F \geq 0$ for any complex channel vector $\boldsymbol{c}$, $\mathbf{T}_F$ is positive semi-definite and its eigenvalues are all non-negative. Denote the positive eigenvalues of $\mathbf{T}_F$ as $\lambda_F(i)$, $i = 1, 2, \ldots, r_F$, where r_F is the rank of $\mathbf{T}_F$. We have

$$J_F = \text{SNR} \cdot \sum_{i=1}^{r_F} \lambda_F(i) |\tilde{c}(i)|^2, \tag{24}$$

where $\tilde{c}(i)$ is the i-th element of vector $\tilde{\boldsymbol{c}} = \mathbf{P}_F \boldsymbol{c}$. As $\mathbf{P}_F$ is unitary, $\tilde{\boldsymbol{c}}$ has the same distribution as $\boldsymbol{c}$. Denoting $\lambda_{F,min} = \min\{\lambda_F(1), \lambda_F(2), \ldots, \lambda_F(r_F)\}$ and

$$J_{F,min} = \text{SNR} \cdot \lambda_{F,min} \sum_{i=1}^{r_F} |\tilde{c}(i)|^2, \tag{25}$$

we have

$$\Pr\{J_F < \delta\} \leq \Pr\{J_{F,min} < \delta\}. \tag{26}$$

Next, we show $\Pr\{J_{F,min} < \delta\} < \Pr\{J_o < \delta\}$ for small δ. $J_{F,min}$ is a chi-squared distributed random variable with $2r_F$ degrees of freedom. The PDF of $J_{F,min}$ is given by [29, Eq. (2.1-110)]

$$f_{F,min}(x) = \frac{1}{(r_F - 1)! \rho_{min}^{r_F}} x^{r_F - 1} e^{-\frac{x}{\rho_{min}}}, \tag{27}$$

where $\rho_{min} = \text{SNR} \cdot \frac{\lambda_{F,min}}{L_c}$. It is straightforward that $r_F > 1$, thus

$$\lim_{x \to 0} f_{F,min}(x) = 0. \tag{28}$$

A similar processing could be performed on J_o and it can be shown that J_o is a chi-squared distributed random variable with 2 degrees of freedom (the rank of $\mathbf{T}_o$ is 1 and it has a single positive eigenvalue that equals to L_c). It can be shown that the PDF of J_o is given by

$$f_o(x) = \frac{1}{\rho_o} e^{-\frac{x}{\rho_o}}, \tag{29}$$

where $\rho_o = \text{SNR}$. We have

$$\lim_{x \to 0} f_o(x) = \frac{1}{\rho_o} > 0. \tag{30}$$

Having (28) and (30) and noticing that $f_{F,min}(x)$ and $f_o(x)$ are *continuous* functions, we have

$$\Pr\{J_{F,min} < \delta\} < \Pr\{J_o < \delta\}, \text{for small } \delta. \tag{31}$$

Combining (26), we finally proved

$$\Pr\{J_F < \delta\} < \Pr\{J_o < \delta\}, \text{for small } \delta. \tag{32}$$

Acknowledgment

The authors would like to thank the anonymous reviewers for their valuable suggestions to improve our paper.

References

[1] B. F. Boroujeny, "OFDM versus filter bank multicarrier," *IEEE Signal Process. Mag.*, vol. 28, no. 3, pp. 92–112, May 2011.
[2] F. Schaich and T. Wild, "Waveform contenders for 5G—OFDM vs. FBMC vs. UFMC," in *Proc. Int. Symp. Commun., Control Signal Process.*, Athens, Greece, May 2014, pp. 457–460.
[3] T. Yunzheng, L. Long, L. Shang, and Z. Zhi, "A survey: Several technologies of non-orthogonal transmission for 5G," *China Commun.*, vol. 12, no. 10, pp. 1–15, Oct. 2015.
[4] F. Schaich, T. Wild, and Y. Chen, "Waveform contenders for 5G—Suitability for short packet and low latency transmissions," in *Proc. IEEE 79th Veh. Technol. Conf. (VTC Spring)*, Seoul, South Korea, May 2014, pp. 1–5.
[5] A. Viholainen, T. H. Stitz, J. Alhava, T. Ihalainen, and M. Renfors, "Complex modulated critically sampled filter banks based on cosine and sine modulation," in *Proc. IEEE Int. Symp. Circuits Syst.*, vol. 1. Phoenix-Scottsdale, AZ, USA, May 2002, pp. 833–836.
[6] A. I. Pérez-Neira *et al.*, "MIMO signal processing in offset-QAM based filter bank multicarrier systems," *IEEE Trans. Signal Process.*, vol. 64, no. 21, pp. 5733–5762, Nov. 2016.
[7] R. Zakaria and D. Le Ruyet, "A novel filter-bank multicarrier scheme to mitigate the intrinsic interference: Application to MIMO systems," *IEEE Trans. Wireless Commun.*, vol. 11, no. 3, pp. 1112–1123, Mar. 2012.
[8] J. Dou, Z. Zhang, J. Dang, L. Wu, Y. Wei, and C. Sun, "Properties and achievable data rate of a cyclic prefix based imperfect reconstruction filter bank multiple access system," *IET Commun.*, vol. 10, no. 17, pp. 2427–2434, Nov. 2016.

[9] J. Dang, M. Guo, Z. Zhang, and L. Wu, "Imperfect reconstructed filter bank multiple access system using wide-banded subbands," in *Proc. IEEE Veh. Technol. Conf. (VTC Spring)*, Sydney, NSW, Australia, Jun. 2017, pp. 1–6.
[10] R. Razavi, P. Xiao, and R. Tafazolli, "Information theoretic analysis of OFDM/OQAM with utilized intrinsic interference," *IEEE Signal Process. Lett.*, vol. 22, no. 5, pp. 618–622, May 2015.
[11] G. Ndo, H. Lin, and P. Siohan, "FBMC/OQAM equalization: Exploiting the imaginary interference," in *Proc. IEEE 23rd Int. Symp. Pers., Indoor Mobile Radio Commun.*, Sydney, NSW, Australia, Sep. 2012, pp. 2359–2364.
[12] R. Zakaria and D. L. Ruyet, "Intrinsic interference reduction in a filter bank-based multicarrier using QAM modulation," *Phys. Commun.*, vol. 11, pp. 15–24, Jun. 2014.
[13] D. Na and K. Choi, "Intrinsic ICI-free alamouti coded FBMC," *IEEE Commun. Lett.*, vol. 20, no. 10, pp. 1971–1974, Oct. 2016.
[14] P. Siohan, C. Siclet, and N. Lacaille, "Analysis and design of OFDM/OQAM systems based on filterbank theory," *IEEE Trans. Signal Process.*, vol. 50, no. 5, pp. 1170–1183, May 2002.
[15] J. Alhava and M. Renfors, "Exponentially-modulated filter bank-based transmultiplexer," in *Proc. IEEE Int. Symp. Circuits Syst.*, vol. 4. Bangkok, Thailand, May 2003, pp. 233–236.
[16] A. Viholainen *et al.* (Jan. 2009). *Prototype Filter and Structure Optimization, Deliverable D5.1, PHYDYAS ICT Project*. [Online]. Available: http://www.ictphydyas.org/delivrables/PHYDYAS-D5-1.pdf/view
[17] J. Alhava and M. Renfors, "Recursive algorithms for modulated and extended lapped transforms," *IEEE Trans. Circuits Syst. I, Reg. Papers*, vol. 61, no. 1, pp. 191–201, Jan. 2014.
[18] S. W. A. Bergen, "A design method for cosine-modulated filter banks using weighted constrained-least-squares filters," *Digit. Signal Process.*, vol. 18, no. 3, pp. 282–290, May 2008.
[19] J. Louveaux *et al.* (Jul. 2008). *Equalization and Demodulation in the Receiver (Single Antenna), Deliverable D3.1, PHYDYAS ICT Project*. [Online]. Available: http://www.ict-phydyas.org/delivrables/PHYDYAS-D3.1.pdf/view
[20] P. P. Vaidyanathan, *Multirate Systems and Filter Banks*. Englewood Cliffs, NJ, USA: Prentice-Hall, 1993.
[21] S. Koslowski and F. K. Jondral, "SIC-MMSE detection for filter bank multicarrier systems," in *Proc. IEEE Veh. Technol. Conf.*, Boston, MA, USA, Sep. 2015, pp. 1–2.
[22] D. Tse and P. Viswanath, *Fundamentals of Wireless Communication*. New York, NY, USA: Cambridge Univ. Press, 2005.
[23] L. G. Baltar, I. Slim, and J. A. Nossek, "Efficient filter bank multicarrier realizations for 5G," in *Proc. IEEE Int. Symp. Circuits Syst.*, Lisbon, Portugal, May 2015, pp. 2608–2611.
[24] J. Nadal, C. A. Nour, and A. Baghdadi, "Low-complexity pipelined architecture for FBMC/OQAM transmitter," *IEEE Trans. Circuits Syst. II, Exp. Briefs*, vol. 63, no. 1, pp. 19–23, Jan. 2016.
[25] J. Dang and Z. Zhang, "Efficient implementation of time domain equalizer for DMT/OFDM systems," in *Proc. IEEE Int. Conf. Commun. Technol.*, Nanjing, China, Nov. 2010, pp. 450–453.
[26] I. Ito and H. Kiya, "A computing method for linear convolution in the DCT domain," in *Proc. 19th Eur. Signal Process. Conf.*, vol. 2. Barcelona, Spain, Aug. 2011, pp. 323–327.
[27] M. Renfors, J. Yli-Kaakinen, and F. J. Harris, "Analysis and design of efficient and flexible fast-convolution based multirate filter banks," *IEEE Trans. Signal Process.*, vol. 62, no. 15, pp. 3768–3783, Aug. 2014.
[28] K. S. Ahn and R. W. Heath, "Performance analysis of maximum ratio combining with imperfect channel estimation in the presence of cochannel interferences," *IEEE Trans. Wireless Commun.*, vol. 8, no. 3, pp. 1080–1085, Mar. 2009.
[29] J. G. Proakis, *Digital Communications*, 4th ed. New York, NY, USA: McGraw-Hill, 2002.

Jian Dang (M'13) received the B.S. degree in information engineering and the Ph.D. degree in information and communications engineering from Southeast University, Nanjing, China, in 2007 and 2013, respectively. From 2010 to 2012, he was with the Department of Electrical and Computer Engineering, University of Florida, Gainesville, FL, USA, as a Visiting Scholar. Since 2013, he has been a Lecturer with the National Mobile Communications Research Laboratory, Southeast University. His current research interests include signal processing in wireless communications, non-orthogonal multiple access schemes, and visible light communications.

Zaichen Zhang (SM'15) received the B.S. and M.S. degrees in electrical and information engineering from Southeast University, Nanjing, China, in 1996 and 1999, respectively, and Ph.D. degree in electrical and electronic engineering from The University of Hong Kong in 2002. From 2002 to 2004, he was a Post-Doctoral Fellow with the National Mobile Communications Research Laboratory, Southeast University, where he is currently a Professor. He is also a Visiting Professor with Nantong University, Nantong, China. His current research interests include ultra-wideband technology, visible light communications, and new generation wireless communication systems.

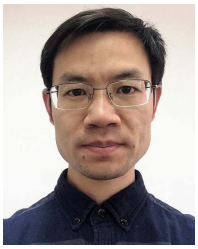

Liang Wu (M'13) received the B.S., M.S., and Ph.D. degrees from the School of Information Science and Engineering, Southeast University, Nanjing, China, in 2007, 2010, and 2013, respectively. From 2011 to 2013, he was with the School of Electrical Engineering and Computer Science, Oregon State University, as a Visiting Student. He is currently a Lecturer with the National Mobile Communications Research Laboratory, Southeast University, Nanjing, China. His current research interests include indoor optical wireless communications, multiple input and multiple output wireless communication systems, and interference alignment.

Yongpeng Wu (S'08–M'13–SM'17) received the B.S. degree in telecommunication engineering from Wuhan University, Wuhan, China, in 2007, the Ph.D. degree in communication and signal processing from the National Mobile Communications Research Laboratory, Southeast University, Nanjing, China, in 2013. He is currently a Research Professor (tenure-track) with the Shanghai Key Laboratory of Navigation and Location-Based Services, Shanghai Jiao Tong University, China. Previously, he was a Senior Research Fellow with the Institute for Communications Engineering, Technical University of Munich, Germany, and the Humboldt Research Fellow and the Senior Research Fellow with the Institute for Digital Communications, University Erlangen-Nürnberg, Germany. During his Ph.D. studies, he conducted cooperative research with the Department of Electrical Engineering, Missouri University of Science and Technology, USA. His current research interests include massive MIMO/MIMO systems, physical layer security, signal processing for wireless communications, and multivariate statistical theory. He was awarded the IEEE Student Travel Grants for IEEE International Conference on Communications 2010, the Alexander von Humboldt Fellowship in 2014, the Travel Grants for IEEE Communication Theory Workshop 2016, and the Excellent Doctoral Thesis Awards of China Communications Society 2016. He was an Exemplary Reviewer of the IEEE TRANSACTIONS ON COMMUNICATIONS in 2015 and 2016, respectively. He is the Lead Guest Editor for the upcoming special issue Physical Layer Security for 5G Wireless Networks of the IEEE JOURNAL ON SELECTED AREAS IN COMMUNICATIONS. He is currently an Editor of the IEEE ACCESS and the IEEE COMMUNICATIONS LETTERS. He has been a TPC member of various conferences, including Globecom, ICC, VTC, and PIMRC.